

Feature Distillation Interaction Weighting Network for Lightweight Image Super-Resolution

Guangwei Gao^{1†}, Wenjie Li^{1†}, Juncheng Li^{2*}, Fei Wu¹, Huimin Lu³, Yi Yu⁴
¹Nanjing University of Posts and Telecommunications ²The Chinese University of Hong Kong
³Kyushu Institute of Technology ⁴National Institute of Informatics

Background

SR aims to reconstruct a high-resolution (HR) image from a low-resolution (LR) image. However, most existing SR models are often accompanied by a large number of model parameters and large calculation costs, which limits their applications on mobile devices.

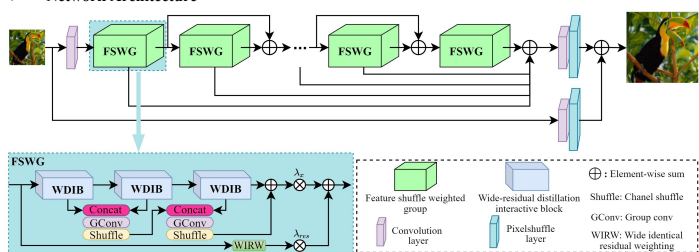
- We aim to explore a lightweight and efficient SR model.
- We aim to solve the problem of how to make full use of intermediate features.

Contributions

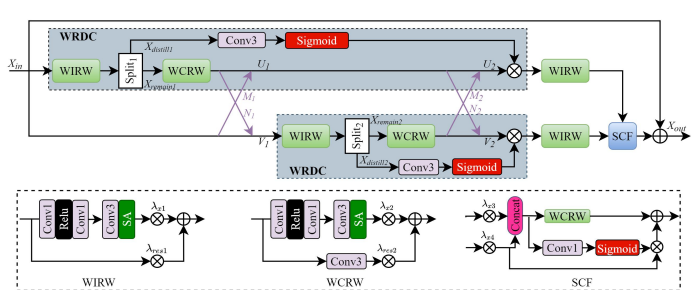
- We propose a wide-residual attention weighting unit for lightweight SISR, which has stronger feature distillation capabilities than ordinary residual blocks.
- We propose a novel Self-Calibration Fusion module to replace the traditional concatenate operation for efficient feature interaction and fusion, which can aggregate more representative features and self-calibrate the input and output features.
- We propose a Wide-Residual Distillation Connection framework, which connects the coarse and distilled fine features within the module and allows features from different scales to interact with each other.
- We design a Feature Shuffle Weighted Group for pairwise feature fusion, which consists of interactional WDIBs. Meanwhile, it serves as a basic component of our proposed model.

Method

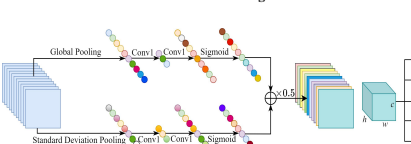
Network Architecture



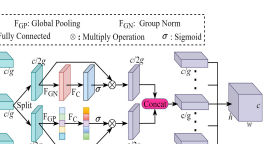
Wide-residual Distillation Interaction Block



Combination Coefficient Learning



Shuffle Attention



Analysis

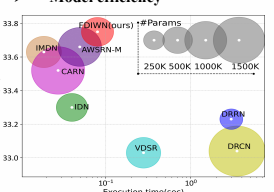
The combination structure of WDIB

| Method | BI | WIRW | Params | Multi-adds | PSNR | SSIM |
|----------|----|------|--------|------------|--------------|---------------|
| Baseline | × | × | 215K | 22.0G | 27.81 | 0.9598 |
| FDIWN | ✓ | × | 225K | 24.4G | 37.85 | 0.9600 |
| FDIWN | ✓ | ✓ | 230K | 24.4G | 37.88 | 0.9600 |

The effectiveness of WRDC and SCF

| Method | WR | DC | SCF | Params | Multi-adds | PSNR | SSIM |
|-----------|----|----|-----|--------|------------|--------------|---------------|
| Baseline1 | × | × | × | 59K | 3.3G | 37.52 | 0.9587 |
| Baseline2 | × | × | × | 59K | 4.9G | 37.53 | 0.9589 |
| FDIWN | × | × | × | 89K | 6.5G | 37.58 | 0.9591 |
| FDIWN | × | × | × | 65K | 6.5G | 37.59 | 0.9590 |
| FDIWN | × | × | × | 96K | 9.7G | 37.64 | 0.9592 |

Model efficiency



Quantitative Comparisons

| Algorithm | Scale | Params | Multi-adds | Set5 | | Set14 | | BSD100 | | Urban100 | |
|--------------------------------------|-------|--------|------------|--------------|---------------|--------------|---------------|--------------|---------------|--------------|---------------|
| | | | | PSNR | SSIM | PSNR | SSIM | PSNR | SSIM | PSNR | SSIM |
| SRCNN (Dong et al. 2015) | × | 57K | 52.7G | 32.75 | 0.9090 | 29.30 | 0.8215 | 28.41 | 0.7863 | 26.24 | 0.7889 |
| FSRCNN (Dong, Loy, and Tang 2016) | × | 12K | 5.0G | 33.16 | 0.9140 | 29.43 | 0.8242 | 28.53 | 0.7910 | 26.43 | 0.8080 |
| VDSR (Kim, Lee, and Lee 2016a) | × | 665K | 612.6G | 33.67 | 0.9210 | 29.78 | 0.8320 | 28.83 | 0.7990 | 27.14 | 0.8290 |
| DRCN (Kim, Lee, and Lee 2016b) | × | 174K | 17974.3G | 33.82 | 0.9226 | 29.76 | 0.8311 | 28.80 | 0.7963 | 27.15 | 0.8276 |
| IDN (Hui, Wang, and Gao 2018) | × | 590K | 105.6G | 34.11 | 0.9253 | 29.99 | 0.8354 | 28.95 | 0.8013 | 27.42 | 0.8359 |
| CARN (Ahm, Kang, and Sohn 2018) | × | 1413K | 116.6G | 33.99 | 0.9236 | 30.29 | 0.8407 | 29.06 | 0.8034 | 28.06 | 0.8493 |
| IMDN (Hui et al. 2019) | × | 703K | 71.5G | 34.36 | 0.9270 | 30.32 | 0.8417 | 29.09 | 0.8046 | 28.17 | 0.8519 |
| AWSRN-M (Wang, Li, and Shi 2019) | × | 1413K | 116.6G | 34.42 | 0.9275 | 30.32 | 0.8419 | 29.13 | 0.8059 | 28.26 | 0.8545 |
| MADNet (Lan et al. 2020) | × | 930K | 88.4G | 34.16 | 0.9253 | 30.21 | 0.8398 | 28.98 | 0.8023 | 27.77 | 0.8439 |
| RFN (Liu, Tang, and Wu 2020) | × | 541K | 55.4G | 34.41 | 0.9273 | 30.34 | 0.8420 | 29.09 | 0.8050 | 28.21 | 0.8525 |
| MAFSRN (Muguet et al. 2020) | × | 418K | 44.2G | 34.32 | 0.9269 | 30.35 | 0.8429 | 29.09 | 0.8052 | 28.13 | 0.8521 |
| LAPAR-A (Li et al. 2021) | × | 591K | 114G | 34.36 | 0.9267 | 30.34 | 0.8421 | 29.11 | 0.8054 | 28.15 | 0.8523 |
| FDIWN-M (Ours) | × | 446K | 35.9 G | 34.46 | 0.9274 | 30.35 | 0.8423 | 29.10 | 0.8051 | 28.16 | 0.8528 |
| FDIWN (Ours) | × | 645K | 51.5G | 34.52 | 0.9281 | 30.42 | 0.8438 | 29.14 | 0.8065 | 28.36 | 0.8567 |
| SRCNN (Dong et al. 2015) | × | 57K | 52.7G | 30.48 | 0.8628 | 27.59 | 0.7503 | 26.90 | 0.7101 | 24.52 | 0.7221 |
| FSRCNN (Dong, Loy, and Tang 2016) | × | 12K | 4.6G | 30.71 | 0.8657 | 27.59 | 0.7535 | 26.98 | 0.7150 | 24.62 | 0.7280 |
| VDSR (Kim, Lee, and Lee 2016a) | × | 665K | 612.6G | 31.35 | 0.8838 | 28.01 | 0.7674 | 27.29 | 0.7251 | 25.18 | 0.7524 |
| DRCN (Kim, Lee, and Lee 2016b) | × | 174K | 17974.3G | 31.53 | 0.8854 | 28.02 | 0.7670 | 27.23 | 0.7233 | 25.14 | 0.7510 |
| LapSRN (Lai et al. 2017) | × | 813K | 149.4G | 31.54 | 0.8850 | 28.19 | 0.7720 | 27.32 | 0.7280 | 25.21 | 0.7560 |
| IDN (Hui, Wang, and Gao 2018) | × | 590K | 81.9G | 31.82 | 0.8903 | 28.25 | 0.7730 | 27.41 | 0.7297 | 25.41 | 0.7632 |
| CARN (Ahm, Kang, and Sohn 2018) | × | 1413K | 116.6G | 31.92 | 0.8903 | 28.26 | 0.7762 | 27.44 | 0.7304 | 25.62 | 0.7694 |
| MAFSRN (Muguet et al. 2020) | × | 1592K | 90.9G | 32.13 | 0.8937 | 28.60 | 0.7806 | 27.58 | 0.7349 | 26.07 | 0.7837 |
| IMDN (Hui et al. 2019) | × | 713K | 71.5G | 32.21 | 0.8948 | 28.58 | 0.7811 | 27.56 | 0.7353 | 26.04 | 0.7838 |
| AWSRN-M (Wang, Li, and Shi 2019) | × | 1254K | 72.0G | 32.21 | 0.8954 | 28.65 | 0.7832 | 27.60 | 0.7368 | 26.15 | 0.7884 |
| MAFSRN (Muguet et al. 2020) | × | 1002K | 54.1G | 31.95 | 0.8917 | 28.40 | 0.7787 | 27.37 | 0.7357 | 25.76 | 0.7746 |
| RFN (Liu, Tang, and Wu 2020) | × | 550K | 31.6G | 32.24 | 0.8952 | 28.61 | 0.7819 | 27.57 | 0.7360 | 26.11 | 0.7858 |
| MAFSRN (Muguet et al. 2020) | × | 441K | 19.3G | 32.18 | 0.8948 | 28.58 | 0.7812 | 27.57 | 0.7361 | 26.04 | 0.7848 |
| MAFSRN (Zhang, Zeng, and Zhang 2021) | × | 603K | 34.7G | 31.92 | 0.8946 | 28.34 | 0.7817 | 27.48 | 0.7393 | 25.81 | 0.7773 |
| FDIWN (Ours) | × | 659K | 94G | 32.15 | 0.8944 | 28.61 | 0.7818 | 27.61 | 0.7366 | 26.14 | 0.7871 |
| LAPAR-A (Li et al. 2021) | × | 603K | 19.6G | 32.17 | 0.8941 | 28.55 | 0.7806 | 27.58 | 0.7364 | 26.02 | 0.7844 |
| FDIWN-M (Ours) | × | 664K | 28.4G | 32.23 | 0.8955 | 28.66 | 0.7829 | 27.62 | 0.7380 | 26.28 | 0.7919 |

Visual Comparisons

